Original

Applying novel fractional order incremental conductance algorithm to design and study the maximum power tracking of small wind power systems

Kuo Nan Yu*, Chih Kang Liao

Department of Electrical Engineering, National Chin-Yi University of Technology, Taichung, Taiwan (R.O.C.)

Abstract

The maximum power point tracking is a very important scheme of many renewable energy. It can increase the power efficiency. However, many traditional methods has defects for the applications. This study proposed a novel fractional order incremental conductance algorithm (FOINC) for the maximum power point tracking design of small wind power systems. The proposed method is prompt in the transient of maximum power point tracking and has good steady-state response. Moreover, it can increase the maximum power tracking efficiency of system without changing the wind power system equipments. The comparison between the traditional incremental conductance method (INC) and Perturbation and Observation (P&O) proved the reliability and effectiveness of the proposed method.

1. Introduction

The renewable energy source is being developed actively in various countries in recent years, among all the available renewable energy sources, the solar energy and wind power have attracted most attention. The wind power is very attractive, because it converts wind energy into kinetic energy, the vanes guide the generator to rotate, it is one of the cleanest energy sources. At present, the PMSG is one of the most frequently used wind turbines for compactness, high power density, low maintenance cost and easy control (Barakati et al., 2005; Jazaeri et al., 2012; Dumnic et al., 2012). The real environment has different wind speed conditions, the wind turbine will have different power characteristic curves, so the Maximum Power Point Tracking (MPPT) is required, so that the output of wind power system is kept at maximum power in different wind speed conditions.

Many MPPT technologies have been implemented in wind power systems in previous literatures, such as Incremental Conductance method (INC) (Kish et al., 2012; Faraji et al., 2014; Sera et al., 2013), P&O (Sera et al., 2013; Mahdi et al., 2012;

Femia et al., 2004), and Hill-Climbing Search Algorithm (HCS) (Raza Kazmi et al., 2011; Yamakura & Kesamaru, 2012). However, most of wind power system control depends on wind speed sensing element, and this type of system needs additional wind speed sensor, so that it is confined to the cost and complexity of sensor (Koutroulis & Kalaitzakis, 2006). The FOINC proposed in this paper only captures the voltage and current of PGMG after the full-bridge rectifier converts the AC generated by the generator into DC. The DC/DC converter as booster adjusts the duty ratio, and the switching pulse width duty cycle of booster is adjusted by algorithm, so as to maximize the output power.

As compared with INC and P&O, the FOINC maximum power tracking controller proposed in this paper is prompt in the transient of MPPT and has good steady-state response. In the real environment, the module life loss resulted from power waveform oscillation can be reduced, the output efficiency of wind turbine is increased and the lost cost is reduced. In other words, the proposed method is practicable for small wind power systems.

2. Brief introduction to wind power systems

In terms of the acquisition of wind energy, the air flow generates air pressure to rotate the vanes to capture the kinetic

* Corresponding author.
  E-mail address: yukn@ncut.edu.tw (K.N. Yu).

energy of wind. Then it is converted into useful kinetic energy or mechanical energy. The energy is contained in the wind, and the rotor blades rotate in wind. Under the effect of aerodynamic force, the vanes generate torque. The power $P_{\omega m}$ generated by wind turbine is expressed as equation (1) (Hau, 2005):

$$P_{\omega m} = \frac{1}{2} \pi \rho C_p R^2 V_\omega^3 \qquad (1)$$

where ρ is the air density, R is the blade radius, V_ω is the wind speed, C_p is the coefficient of performance of wind turbine. C_p includes the blade tip speed ratio λ. λ is defined as the relationship between blade tip speed and wind speed, expressed as equation (2):

$$\lambda = \frac{T\omega_m}{v_\omega} \qquad (2)$$

where ω_m is the blade rotation speed. Figure 1 shows the power characteristic curves in different wind speed conditions (Nakamura et al., 2002).

2.1. Wind power system architecture

The wind power system architecture proposed in this paper is shown in Figure 2, the wind turbine is coupled to the PMSG directly, connected to a set of rectifier, converting the AC of generator into DC. The DC voltage and current signals are obtained, and the signals are connected to the DC-DC boost converter. The MPPT is used to control signals and adjust the duty cycle of switching pulse width modulation (PWM). Finally, the DC-DC boost converter is connected to the load, and the system output power is measured. The basic structure of the converter is shown in Figure 3. When the switch is "on", the wind power system charges the inductor via the switch. When the switch is "off", the wind power system releases the inductance energy to the load via diode. The output voltage and current can be changed by different input voltages and currents by adjusting the duty ratio. When
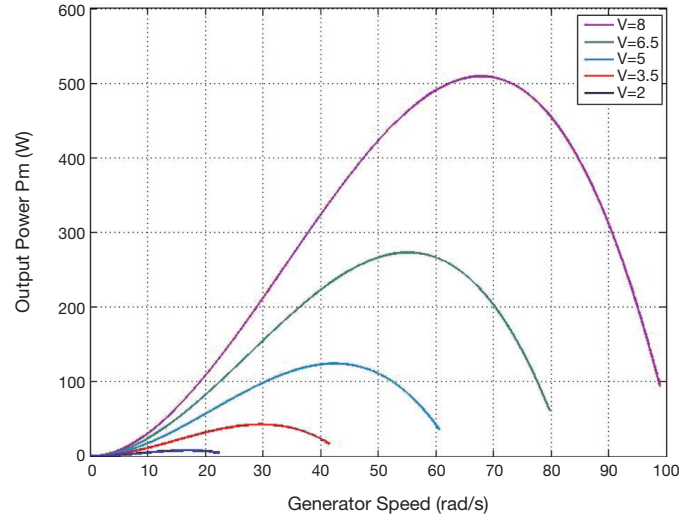

Fig. 1. Power characteristic curves.

the switch is off t_{off} and on t_{on}, the current through inductor can be expressed as:

$$\text{Switch on } t_{on} : \Delta I_L^+ = \frac{V_i}{L} t_{on} \qquad (3)$$

$$\text{Switch off } t_{off} : \Delta I_L^- = \frac{V_i - V_o}{L} t_{off} \qquad (4)$$

Duty ratio (D) of control switch is:

$$D = \frac{t_{on}}{t_{on} + t_{off}} = \frac{t_{on}}{T_d} \qquad (5)$$

As the one-cycle voltage variation of inductor is 0, i.e. $\Delta I_L^+ = \Delta I_L^-$.

The equation of output voltage V_o can be obtained:

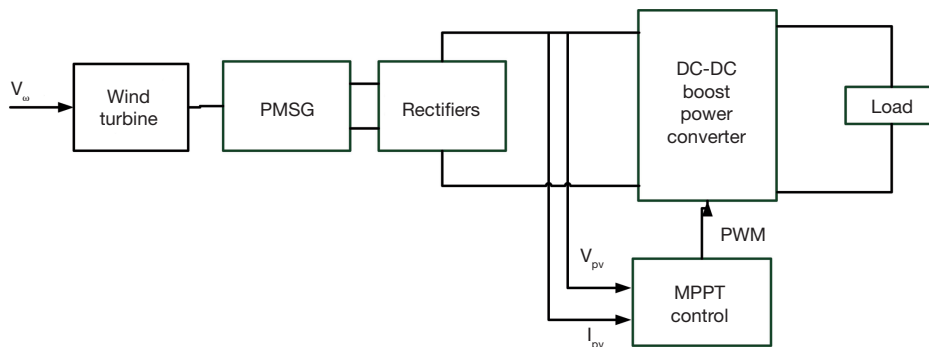$$V_o = V_i \frac{t_{on} + t_{off}}{t_{on}} = \frac{V_i}{1-D} \qquad (6)$$
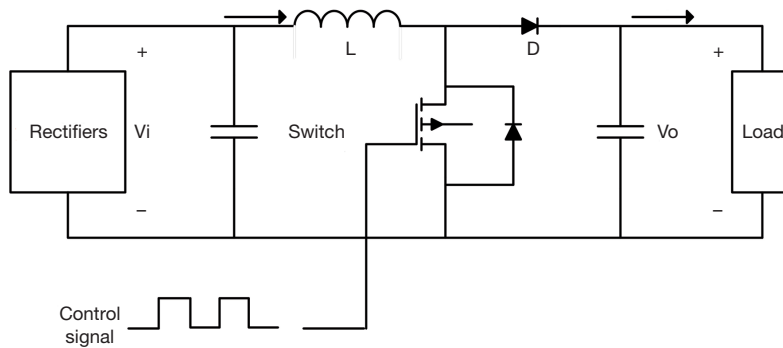

Fig. 2. Wind power system architecture.
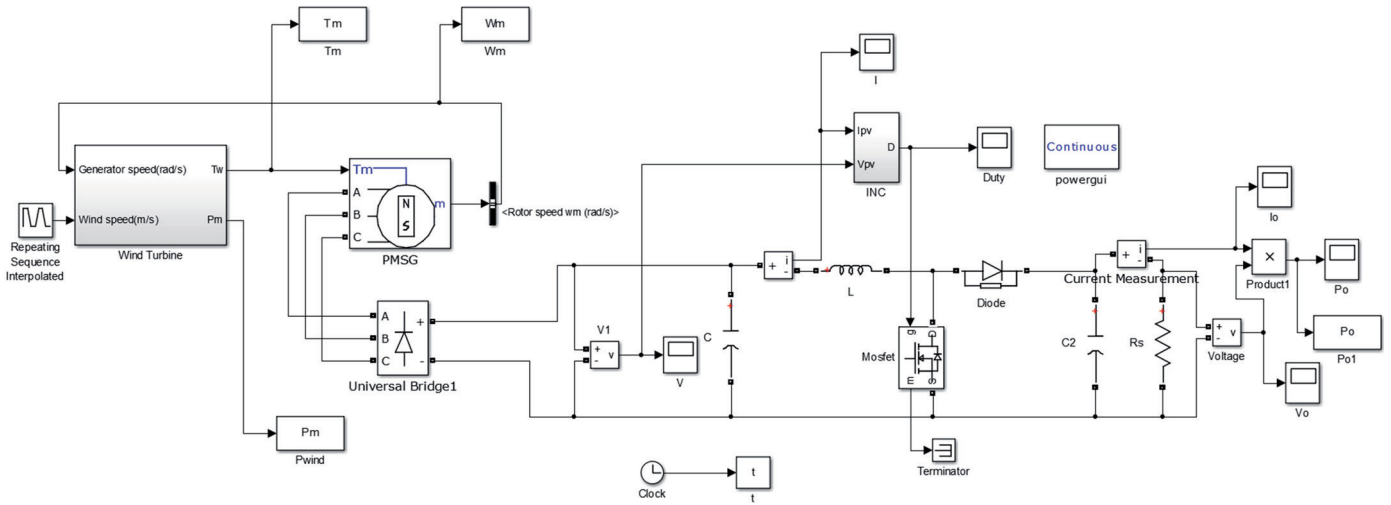
Fig. 3. Boost-converter equivalent circuit diagram.

Fig. 4. Simulation diagram of PMSG wind power system.

3. Design of algorithm and control method

This study used MATLAB R2010a Simulink to build the simulated small wind power system architecture and to design the control method. Figure 4 shows the simulation diagram of the wind power system. The module FOINC can be replaced by different MPPTs for duty cycle control of different switching pulse adjustment control methods.

3.1. Hill-Climbing Search (HCS)

The most frequently used algorithm in wind power systems at variable wind speed is the HCS. This algorithm looks for the optimum speed of wind turbines according to the perturbation of wind speed to complete MPPT. The improved HCS can be derived from this algorithm. The detailed algorithm flowchart and content can be seen in literature (Dalala et al., 2013).

3.2. Perturbation and Observation (P&O)

The P&O is one of the most extensively used methods in recent years. Its advantages include simple architecture, fewer

required parameters and being free from atmospheric influence. The terminal voltage and output power of wind turbine are changed by changing the duty cycle *D*, and whether the changed output power increases continuously or not is observed. The power point on the left or right of curve is judged according to the input voltage. Finally, whether the duty cycle *D* keeps changing in the same direction or not is determined. The maximum power point can be reached by such repeated perturbation, observation and comparison. However, this method uses periodic perturbation, so there is oscillation at maximum power point, resulting in unnecessary power loss of system.

3.3. Incremental Conductance method (INC)

The INC is based on power-voltage (*P – V*) curve of solar cell, equations (7) or (8) must be met at maximum power point:

$$\frac{dP}{dV} = 0 \tag{7}$$

$$\frac{dI}{dV} \approx -\frac{I - I_o}{V - V_o} = -\frac{\Delta I}{\Delta V} \tag{8}$$

where I_o and V_o are the current and voltage captured at previous point in time, ΔI and ΔV are the variation of current and voltage in unit time. However, when the method processes MPPT, the offset ΔV determines the speed of reaching the MPP and the perturbation after the MPP is reached. The decision must be made by the user.

3.4. Fractional order incremental conductance method

The fractional-order differentiator is often applied to signal processing, adaptive control, active control, linear and nonlinear feedback control. At present, many computing applications of fractional-order derivative have been proposed, according to the definition of Riemann-Liouville and Grunwald-Letnikov (Igor, 1999; Ma & Hori, 2007; Kenneth & Bertram, 1993). General fractional-order differentiator can be expressed as:

$$D_t^\alpha t^m \approx \frac{\gamma(m+1)}{\gamma(m+1-\alpha)} t^{m-\alpha} \qquad (9)$$

where $\gamma(\ )$ represents the γ function (gamma function), α is the order number of derivative, when its value is $0 < \alpha < 1$, representing the physical phenomenon of fractional order, its application can refer to Tavakoli-Kakhki et al. (2013), Ma and Hori (2007), and Saha et al. (2010).

General fractional-order differentiator can be expressed as equation (9), when the INC is used, equation (8) can be expressed as:

$$\frac{d^\alpha I}{dV^\alpha} \approx \lim_{\Delta V \to 0} \frac{I(V) - \alpha I(V - \Delta V)}{\Delta V^\alpha} \qquad (10)$$

$$\frac{d^\alpha I}{dV^\alpha} \approx \frac{I - \alpha I_0}{(V - V_0)^\alpha} \qquad (11)$$

If $\alpha > 0$ in ΔV^α, the geometric interpretation of fractional order can be represented as Figure 5. The slope is a straight line when $\alpha = 1$, i.e. general first derivative. Therefore, $0 < \alpha < 1$ presents the form of fractional-order derivative, approximate to curve form, referring to literature (Shantanu, 2008). The result of using equation (9) in the right half of equation (8) is:

$$\frac{d^\alpha}{dV^\alpha}\left(-\frac{I_o}{V_o}\right) = \left(-\frac{1}{V_o}\right)\frac{d^\alpha I_o}{dV^\alpha} + (-I_o)\frac{d^\alpha V_o^{-1}}{dV^\alpha} \qquad (12)$$

$$= \left(-\frac{1}{V_o}\right)\left(\frac{\gamma(2)}{\gamma(2-\alpha)}\right)(I_o)^{1-\alpha} + \frac{(-I_o)(\gamma(0))}{\gamma(-\alpha)}V_o^{-1-\alpha}$$

where $res(\gamma, -z) = \frac{(-1)^z}{z!}$, $z = 0, -1, -2, -3, \ldots$, and $\gamma(0) = res$ (γ, 0), res represents the residue under complex plane.

The voltage V, current I and power P are used as calculated captured signals in this paper. The variance in voltage and current $\Delta V = V - V_o$, and $\Delta I = I - I_o$, the slope is the slope $\left(\frac{\Delta P}{\Delta V}\right)$
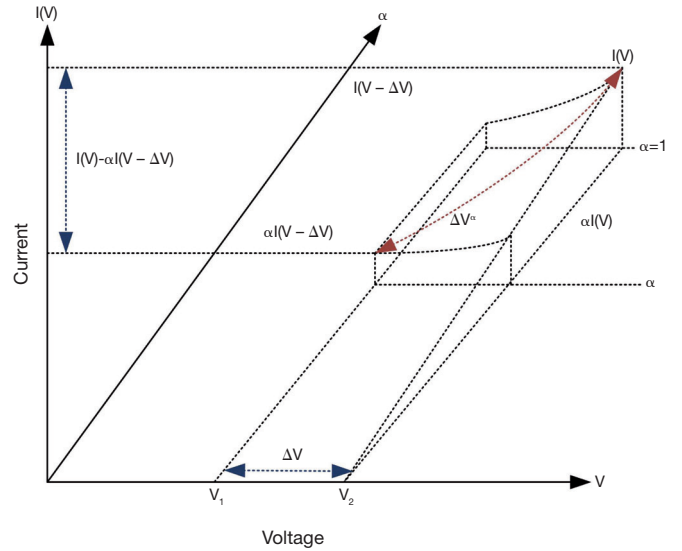

Fig. 5. Geometric interpretation of ΔV in fractional-order differentiator.

of power-voltage curve of wind turbine, and the variation of partial voltage and current of fractional-order differentiator approximates as $d^\alpha I = I - \alpha I_o$, $dV^\alpha = (V - V_o)^\alpha$.

The control flow of FOINC proposed in this paper is shown in Figure 6.

4. Simulation analysis results and comparison

This study used MATLAB R2010a Simulink to build the model and controller of small wind power systems, and proposed the PMSG-based wind power system. The simulation compared the INC and P&O with FOINC proposed in this paper at constant wind speed and variable wind speed.

The first simulated condition is constant wind speed of 12.5 *m/s*, as shown in Figure 7. The INC and P&O and FOINC proposed in this paper are analyzed and compared in this wind speed condition.

As shown in Figure 8, in the constant wind speed, the MPPT speed of FOINC proposed in this paper is better than P&O and INC, and the steady-state response is smoother than P&O and INC, thus reducing unnecessary power loss, and increasing the efficiency, proving the practicability of the proposed method.

The second simulated condition is variable wind speed for test and comparison of algorithms. The wind speed conditions are 12.5 *m/s* and 10 *m/s*, as shown in Figure 9. The INC and P&O and FOINC proposed in this paper are analyzed and compared in the wind speed condition.

As shown in Figure 10, the MPPT speed of FOINC proposed in this paper is better than P&O and INC, and the amplitude in steady-state is steadier than P&O and INC. Therefore, a better response curve can be obtained in the variable wind speed condition, proving the feasibility of the proposed method.
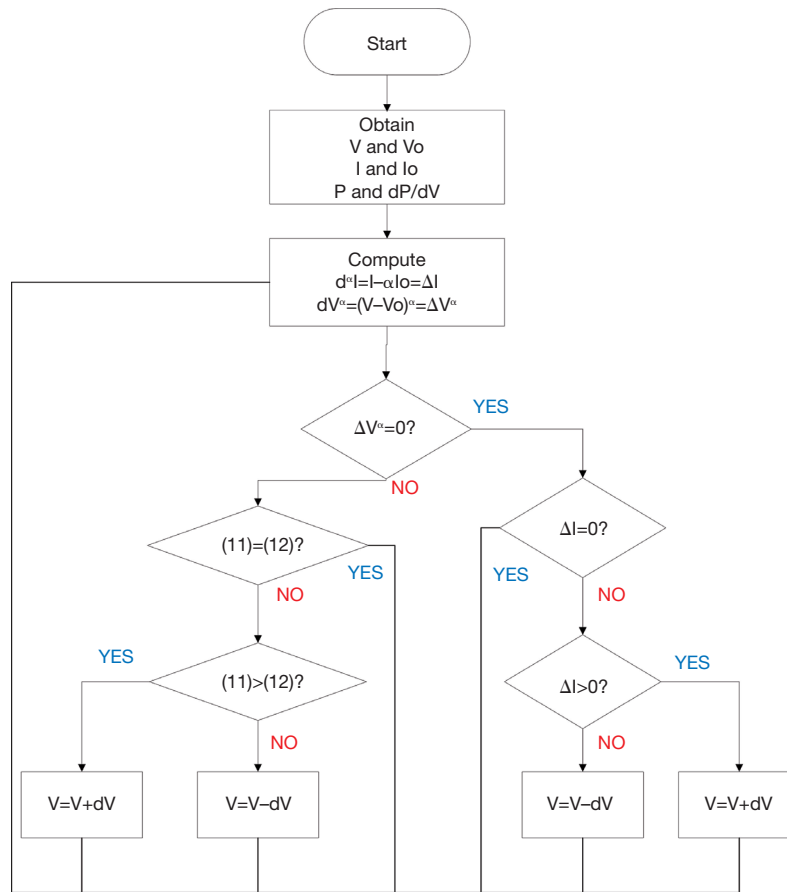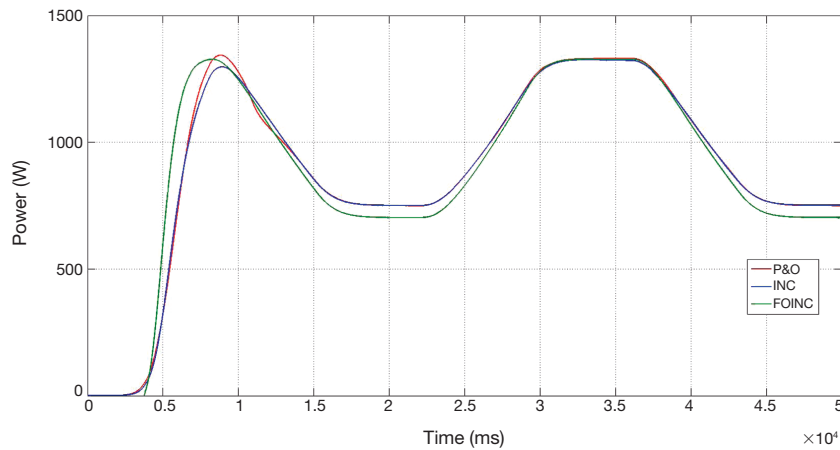
Fig. 6. Algorithm flowchart of FOINC.

Fig. 7. Step input constant wind speed 12.5 *m/s*.

5. Conclusions

The FOINC proposed in this paper can control the algorithm only by capturing the voltage and current generated by the wind power system without adjusting the parameter setting for different systems. The transient tracking is prompt and the perturbation after steady-state is better than existing methods. According to the simulation results, due to fewer required parameters, high speed and good stability, the small wind power system is free from excess sensing elements, so that the cost is reduced. The FOINC proposed in this paper can be applied and implemented to the MPPT of small wind power systems in the future.
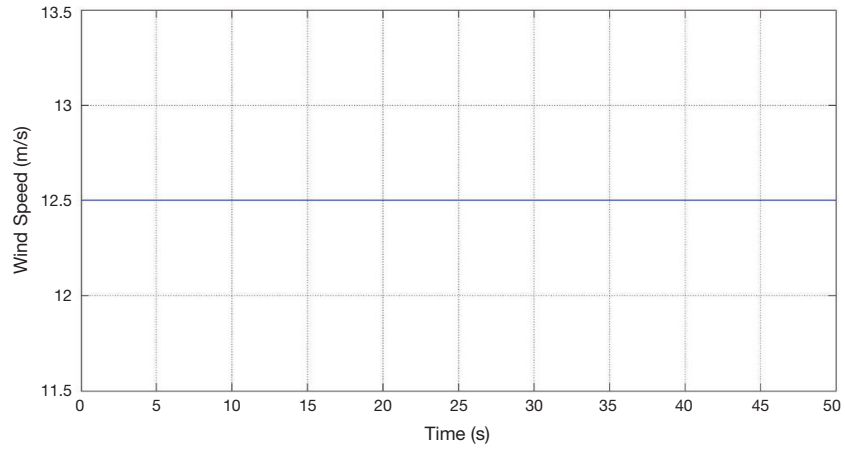
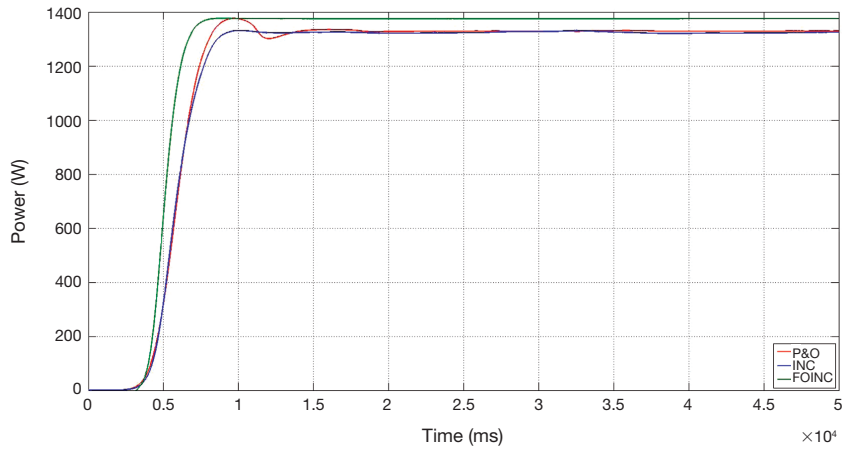Fig. 8. Output dynamic response of P&O, INC and FOINC (constant wind speed).

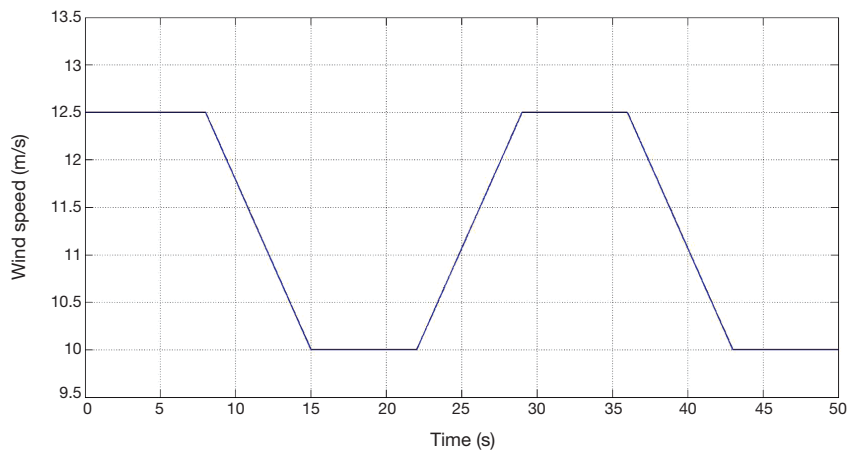Fig. 9. Variance in input wind speed of 12.5 *m/s* and 10 *m/s*.

Fig. 10. Output dynamic response of P&O, INC and FOINC (variable wind speed).

References

Barakati, S.M., Kazerani, M., & Chen, X. (2005). A new wind turbine generationsystem based on matrix converter, in *Proc. IEEE Power Engineering Society General Meeting,* June 12-16 (vol. 3, pp. 2083-2089).

Dalala, Z.M., Zahid, Z.U., Wensong Yu, Younghoon, C., & Jih-Sheng, L. (2013). Design and Analysis of an MPPT Technique for Small-Scale Wind Energy Conversion Systems. *IEEE Transactions on Energy Conversion, 28,* 759-67.

Dumnic, B., Katic, V., Vasic, V., Milicevic, D., & Delimar, M. (2012). An Improved MRAS Based Sensorless Vector Control Method for Wind Power Generator. *Journal of Applied Research and Technology, 10,* 687-679.

Faraji, R., Rouholamini, A., Naji, H.R., Fadaeinedjad, R., & Chavoshian, M.R. (2014). FPGA-based real time incremental conductance maximum power point tracking controller for photovoltaic systems. *IET Power Electron, 7,* 1294-304.

Femia, N., Petrone, G., Spagnuolo, G., & Vitelli, M. (2004). *Optimizing Duty-cycle Perturbation of P&O MPPT Technique.* IEEE TTransactions on Power Electronics Conference, 20-25 June.

Hau, E. (2005). *Wind Turbines: Fundamentals, Technologies, Application, Economics.* Berlin, Germany: Springer.

Jazaeri, M., Samadi, A.A., Najafi, H.R., & Noroozi-Varcheshme, N. (2012). Eigenvalue Analysis of a Network Connected to a Wind Turbine Implemented with a Doubly-Fed Induction Generator (DFIG). *Journal of Applied Research and Technology, 10,* 791-811.

Kenneth S., Miller & Bertram, R. (1993). *An introduction to the fractional calculus and fractional differential equations.* New York: John Wiley & Sons.

Kish, G.J., Lee, J.J., & Lehn, P.W. (2012). Modelling and control of photovoltaic panels utilising the incremental conductance method for maximum power point tracking. *IET Renewable Power Generation, 6,* 259-66.

Koutroulis, E., & Kalaitzakis, K. (2006). Desgin of a Maximum Power Point Tracking System for Wind-Energy-Conversion Applications. *IEEE Industrial Electronics Magazine, 53,* 486-494.

Ma, C., & Hori, Y. (2007). Fractional-order control:theory and applications inmotion control. *IEEE Industrial Electronics Magazine, 1,* 6-16.

Mahdi, A.J., Tang, W.H., & Wu, Q.H. (2012). *Novel Perturbation and Observation Algorithms for Variable-speed Wind Turbine Generator Systems.* Power and Energy Society General Meeting, IEEE, 22-26 July 2012.

Nakamura, T., Morimoto, S., Sanada, M., & Takeda, Y. (2002). *Optimum control of IPMSG for wind generation system.* IEEE Power Conversion Conference (vol. 3, pp. 1435-1440).

Podlubny I. (1999). *Fractional differential equations. Mathematics in science and engineering.* New York: Academic Press.

Raza Kazmi, S.M., Goto, H., Hai-Jiao G., & Ichinokura, O. (2011). A Novel Algorithm for Fast and Efficient Speed-Sensorless Maximum Power Point Tracking in Wind Energy Conversion Systems. *IEEE Industrial Electronics Magazine, 58,* 29-36.

Saha, S., Das, S., Ghosh, R., Goswami, B., Balasubramanian, R., Chandra, A.K., …, & Gupta, A. (2010). Design of a Fractional Order Phase Shaper for Iso-Damped Control of a PHWR Under Step-Back Condition. *IEEE Transactions on Nuclear Science, 57,* 1602-1612.

Sera, D., Mathe, L., Kerekes, T., Spataru, S.V., & Teodorescu, R. (2013). On the Perturb-and-Observe and Incremental Conductance MPPT Methods for PV Systems. *IEEE Journal of Photovoltaics; 3(3):*1070-1078.

Shantanu, D. (2008). *Functional fractional calculus for system identification and controls.* Berlin Heidelberg, New York: Springer.

Tavakoli-Kakhki, M., Haeri, M., & Tavazoei, M.S. (2013). Study on Control Input Energy Efficiency of Fractional Order Control Systems. *IEEE Transactions on Circuits and Systems I-Regular Papers, 3,* 475-482.

Yamakura, S., & Kesamaru, K. (2012). Dynamic Simulation of PMSG Small Wind Turbine Generation System with HCS-MPPT Control. *Electrical Machines and Systems (ICEMS),* 21-24 Oct.